Profiles of Pressure Broadened Spectral Lines in an Arc Plasma

Reda A. El-Koramy and Abd El-Halim A. Turky

Physics Department, Faculty of Science, Assiut University, 71516 Assiut, Egypt

Reprint requests to Dr. R. A. El-K.; E-mail: elkoramy@yahoo.com

Z. Naturforsch. **60a,** 727 – 735 (2005); received July 28, 2005

Spectral analysis of the alkali metals is characterized by pressure profiles. In the present work an electric arc has been used to calibrate the half-width of the intensity used in the construction of the ArI natural line at 4300 Å with a trace of evaporated rubidium at pressures of 1, 2 and 3 atmospheres. The results agree well with those obtained by Kusch's line absorption equation in an electric furnace in the point of view of impact approximation, showing that the widths of the lines have Lorentz shapes. It is found that a simple treatment can be given using the quasi-static approximation of pressure broadening developed by Unsöld. The agreement of the results is good only if the shifts are large. The study shows that the pressure line profile is made up of a sum of dispersion profiles and asymmetric terms which arise from interactions of quadratic Stark effect, commonly assumed to be the force in causing foreign gas broadening.

Key words: Pressure Broadening; Arc Plasma; Lorentz Shapes; Quadratic Stark Effect.

1. Introduction

Pressure broadening of spectral lines arises when an atom, molecule or ion is emitting light in a carrier gas. The study of this phenomenon is necessary for accurate spectroscopic analysis, and it can yield useful information about the conditions in the gas.

Pressure effects of some gases, especially argon, on the second doublet of the principle series of some alkali metals have been reported by Watson and Margenau [1], Ny and Ch'en [2], and Robin and Robin [3]. It has been shown that the relationship between the shift and the density of the gas is more than linear in a restricted pressure range. The various results of other authors [4 – 6] on various other gas-alkali metals combinations in limited pressure ranges have not given a clear picture for theoretical physicists.

Recently other authors [7], using the semi-classical perturbation approach, have calculated the electronic and ionic widths and shifts of several OI spectral lines by quasi-static approximations. The obtained data were compared with the previous work of others [23]. Using Thomson's scattering measurement in an argon arc atmospheric pressure [8], it has been demonstrated that its line width is much greater than the absorption line width of rubidium, so it passes through the Rb filter into the spectrometer. For potassium vapor as perturbation, the Lorentz local-field [9] was used to modify the properties of a dense medium compared to isolated atoms. It has been concluded that it results in the Lorentz-Lorentz shift and a negative delay signal in transient-four wave mixing. A set of new results of the Stark broadening parameters of visible neutral argon lines in a plasma of atmospheric pressure is presented in [10].

Spectral investigations of alkali metal evaporation in a gas plasma have been done theoretically and experimentally [6]. However, no measurements have been reported for the pressure profiles of excited state transitions using an alkali metal as perturber.

In special cases, where a plasma of high particle density is needed, a gas stabilized high pressure arc should be achieved. This could be easily started by a high voltage discharge. In the present work observations are presented which make full use of Kusch's absorption line intensity [11] and statistical [12] theories of pressure broadening to explain the pressure profile of the ArI neutral line at 4300 Å spectral line with a trace of evaporated rubidium as the alkali perturber. The choice of argon and rubidium is motivated by the recent interest in their spectroscopic properties. Because argon is monatomic and relatively heavy, it is often used in diaphragm-type shock tubes. Rubidium, with its high vapour pressure and low ionization potential, has many applications in plasma sources. It should be pointed out here, that, since Stark broadening dominates the Doppler broadening, the line profiles do not depend critically [13] on the electron and ion velocity distributions or the temperature, hence electron densities can be inferred from the line profiles without knowing the plasma temperature precisely.

2. Theory

The frequency dependence of line absorption coefficients is almost never determined by natural broadening alone, except at very low densities and great distances from the line center. Besides natural broadening, Doppler broadening is always present and dominates the shape near the line center at low densities. However, in dense plasmas these universal line broadening mechanisms are often negligible, because the line shapes are strongly influenced by interactions of the radiating atoms or ions with surrounding particles. Then one speaks of pressure broadening. The most important interactions are those between radiating systems and plasma ions or electrons. Because electric fields are involved, this type of broadening is called Stark broadening.

Excited atoms in a plasma are subject to the quadratic Stark effect due to the electric micro-fields generated by slow moving ions, and they experience small changes in their excitation energies. Since the interaction with other energy levels is repulsive, and since there are usually more interacting levels above a given excited level than below, the levels are normally shifted to smaller values. This effect is normally much more pronounced for upper levels of a transition, since its sensitivity to the perturbing electric micro-field is much greater than that of the more tightly bound lower level. Therefore, the transitions are most often shifted to lower frequencies, i. e., they exhibit red shifts and a slight red asymmetry [14]. The distribution of electrical micro-fields in a plasma due to the various ion perturbed configurations not only leads to an effective shift and width, but also introduces asymmetries in the line profile which are superimposed on the symmetrical electron-impact-broadened line shape.

To calculate the phase shift due to an encounter, we will assume that:

- the perturber can be considered as a classical particle;
- the perturber moves on a straight line relative to the atom with an impact parameter;
- no transitions in the atom are produced by the action of the perturber.

Occasionally other interactions must be considered. Interactions with neutral atoms of the same kind as the radiating ones may give rise to resonance broadening, if one of the states in the line has allowed transitions to the ground state, and interactions with other atoms give rise to van der Waals broadening. We have treated the case in which the interaction of a radiating atom with its neighbors consists of a succession of binary collisions. Each of these encounters is assumed to provide a frequency modulation of the form

$$\Delta\omega(r) = \frac{C_n}{r^n}, \tag{1}$$

where r is the mean perturbing distance, C_n is the Stark constant, and the index n depends on the nature of the interaction, values of which are represented as follows:

$n = 2$, linear Stark effect;
$n = 3$, resonance broadening;
$n = 4$, quadratic Stark effect;
$n = 6$, van der Waals interaction.

The relationships between n and the shift $\Delta\lambda_s$ and the half-width $\Delta\lambda_{1/2}$ of the spectral lines for each n are tabulated in [15].

In addition to the above classification of the various pressure broadening mechanisms, there is the division into impact (collision) and quasi-static (statistical) broadening. In the plasma medium, the free electrons and the ions in the gas disturb the atom emitting the light. In order to take into account the effect of electrons and ions simultaneously, we apply the impact theory [16] to the electrons. When a certain ionic field is present, then we take the average result over all ionic fields. Since the effect of the ionic field is usually to split the line into a number of components, we are faced with the problem of applying the impact theory to a number of very close lines which, when broadened by the electrons, will overlap, resulting in an isolated line having a Lorentz shape. So, the line profile is made up of a sum of dispersion profiles and asymmetric terms which arise from interactions of the quadratic Stark effect. The absorption pressure dispersion profile given by Kusch [17] is written as

$$K = \frac{\pi e^2}{m_e c} N_e f \frac{\Delta\lambda_{1/2}}{\left\{\frac{2\pi c}{\lambda^2}\right\}(\Delta\lambda)^2 + \left\{\frac{\Delta\lambda_{1/2}}{2}\right\}^2}, \tag{2}$$

where f is the dimensionless absorption oscillator strength, m_e and N_e are the electronic mass and density, respectively, c is the velocity of light and $\Delta\lambda$ is the displacement from the line center.

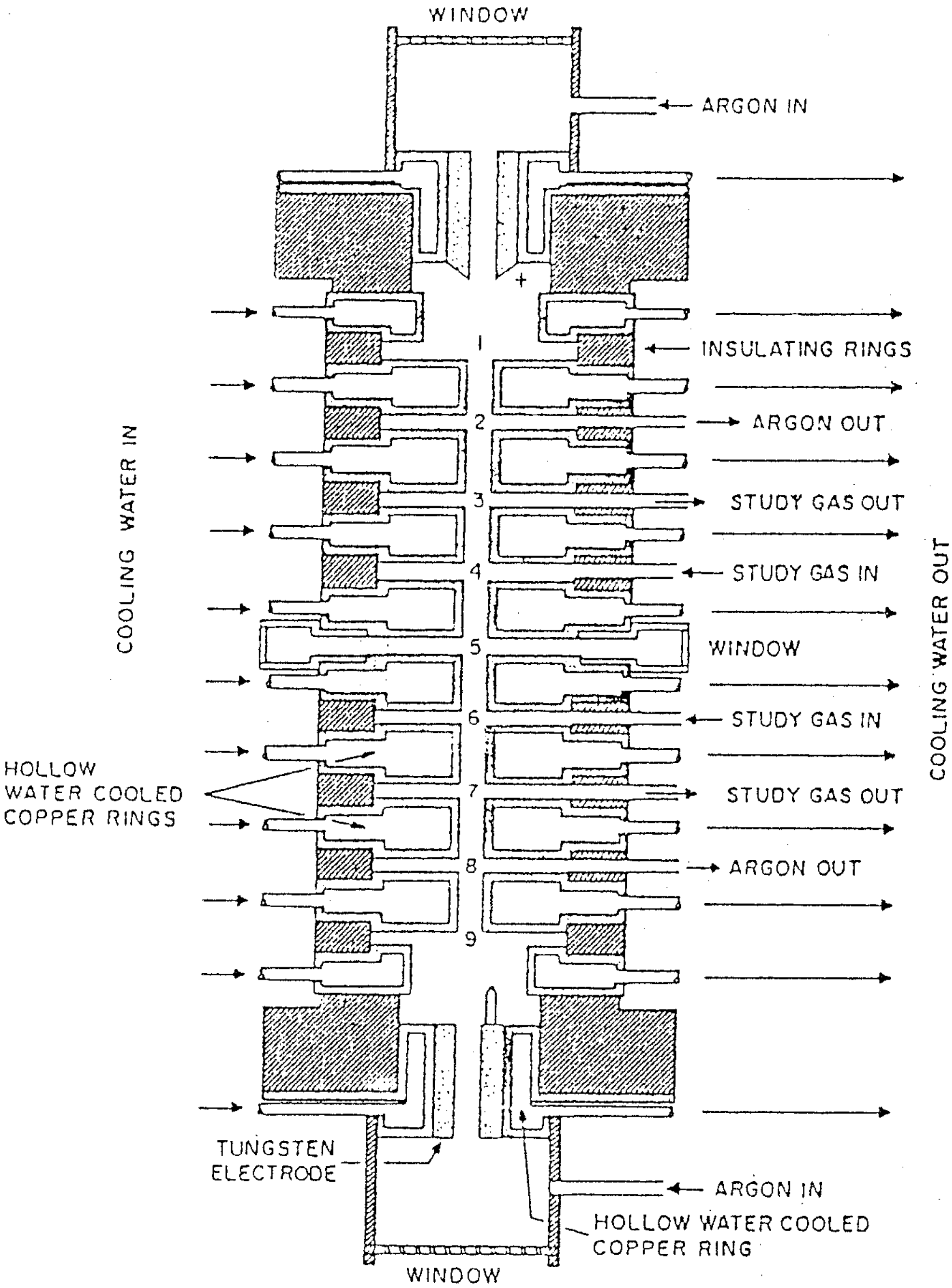

Fig. 1. Schematic diagram of the wall-stabilized arc with tungsten electrodes (from [17]).

On the other hand, if the broadening ions are as heavy as argon, their motion can almost be neglected. Then one can use both the adiabatic and the quasi-static approximation. According to this theory, the electric field of the ions splits the line through the Stark effect. The resulting pattern is then averaged over all electric fields with the appropriate probability distribution. For higher densities, the simplest static theory is to assume the disturbance $\Delta\omega$ as being due only to the nearest neighbour. Introducing the relation (1) and the normal shift $\Delta\omega_o$ corresponding to the mean distance of the particle, where

$$\Delta\omega_o = C_n r_o^{-n} = C_n \left(\frac{4}{3}\pi N_e\right)^{n/3},$$

Unsöld [12] found that the intensity distribution is given by:

$$K_\lambda = \frac{3}{n}\left(\frac{\Delta\omega_o}{\Delta\omega}\right)^{(n+3)/n} \exp\left(-\left(\frac{\Delta\omega_o}{\Delta\omega}\right)^{3/n}\right)\frac{1}{\Delta\omega_o}, \tag{3}$$

which gives an asymmetrical profile for a line. The most important case of interaction in the pressure broadening is the quadratic Stark effect, where $n = 4$.

3. Experimental Set-up and Procedure

Figure 1 shows a schematic diagram of the common wall high stabilized cylindrical cascade arc developed by Wiese et al. [17], in which four tungsten electrodes are used. The local thermal equilibrium was obtained by using stacks of insulated water-cooled copper disks. The ArI 4300 Å spectral line was generated in the arc operated in argon with a trace of evaporated rubidium. The central channel diameter of the arc is 4 mm, its length 48 mm, and the arc current is operated at 60 A through a 60 Ω resistance at a pressure of 1, 2 and 3 atm.

The gas mixture (0.3% Rb vapor and 99.7% Ar) is fed at the midpoint of the arc channel. The desired pressure within the arc is maintained by the aid of manometers. Reabsorption of the line radiation in cooler boundary layers has to be avoided within the aperture in front of the anodes, using a special relay system.

The plasma column of the arc was observed end-on from the anode side, its enlarged image is focused onto the entrance slit of a 2.5-m Ebert type spectrograph with 1200-line/mm holographic grating, yielding a linear dispersion of about 1.6 Å/mm. For measurements of the arc radiation both the entrance and exit slits are set at 45 μm to produce an instrument-limited line width of about 0.1 Å. The electrical equipments are: a photomultiplier tube EMI type 9781-3 No. 14402 and a recorder from Fabric Linsies (Germany).

Deviations from the local thermodynamic equilibrium (LTE) were found to be negligibly small in the investigated interval of the electron density (N_e). N_e

Table 1. Relation between K_λ and $\Delta\lambda$ at $P = 1$ atm.

$\Delta\lambda$, Å	0	0.2	0.4	0.6	0.8	1	1.2	1.4	2
K_λ	0.39	0.33	0.23	0.14	0.09	0.066	0.048	0.037	0.019

Table 2. Relation between K_λ and $\Delta\lambda$ at $P = 2$ atm.

$\Delta\lambda$, Å	0	0.2	0.4	0.6	0.8	1	1.2	1.4	1.6	2
K_λ	1	0.67	0.33	0.18	0.11	0.075	0.057	0.039	0.030	0.019

Table 3. Relation between K_λ and $\Delta\lambda$ at $P = 3$ atm.

$\Delta\lambda$, Å	0	0.2	0.4	0.6	0.8	1	1.2	1.4	1.8	2
K_λ	3.6	1.28	0.43	0.21	0.12	0.076	0.055	0.04	0.031	0.020

is calculated from the empirical relation proposed by Pittman and Fleurier [18]:

$$N_e, \mathrm{m}^{-3} = 3.31(\Delta\lambda_{1/2})^{1.21}\,10^{23},$$

$\Delta\lambda_{1/2}$ is given in nm.

4. Results and Discussion

Taking into consideration that the mobility decreases as the pressure P increases [19], both the half-width and shift decrease too. By the knowledge of $N_e \sim 10^{16}$ cm^{-3}, $f \sim 10^{-4}$, and substituting (2), we have the absorption pressure dispersion profile in the simple form

$$K_\lambda = 9\cdot 10^{-6}\frac{\Delta\lambda_{1/2}}{12.5(\Delta\lambda)^2 + (\Delta\lambda_{1/2})^2}. \tag{4}$$

At $P = 1$ atm, $\Delta\lambda_{1/2} = 1.6$ Å, so (4) becomes

$$K_\lambda = 14.4\cdot 10^{-6}\frac{1}{12.5(\Delta\lambda)^2 + 2.56}. \tag{5}$$

Table 1 shows the relation between K_λ, in its fraction part, and $\Delta\lambda$.

At $P = 2$ atm, the relation between the new half-width and the first one $\left(\frac{\Delta\lambda_{1/2}}{1.6}\right)$ is 0.625 : 1. Then the new $\Delta\lambda_{1/2}$ equals 1 Å, and (4) yields:

$$K_\lambda = 9\cdot 10^{-6}\frac{1}{12.5(\Delta\lambda)^2 + 1}. \tag{6}$$

Table 2 shows this relation in the fraction part.

At $P = 3$ atm, $\left(\frac{\Delta\lambda_{1/2}}{1.6}\right)$ is 0.33 : 1. Then $\Delta\lambda_{1/2} = 0.528$ Å, and (4) becomes

$$K_\lambda = 4.75\cdot 10^{-6}\frac{1}{12.5(\Delta\lambda)^2 + 0.28}. \tag{7}$$

Table 3 shows this relation.

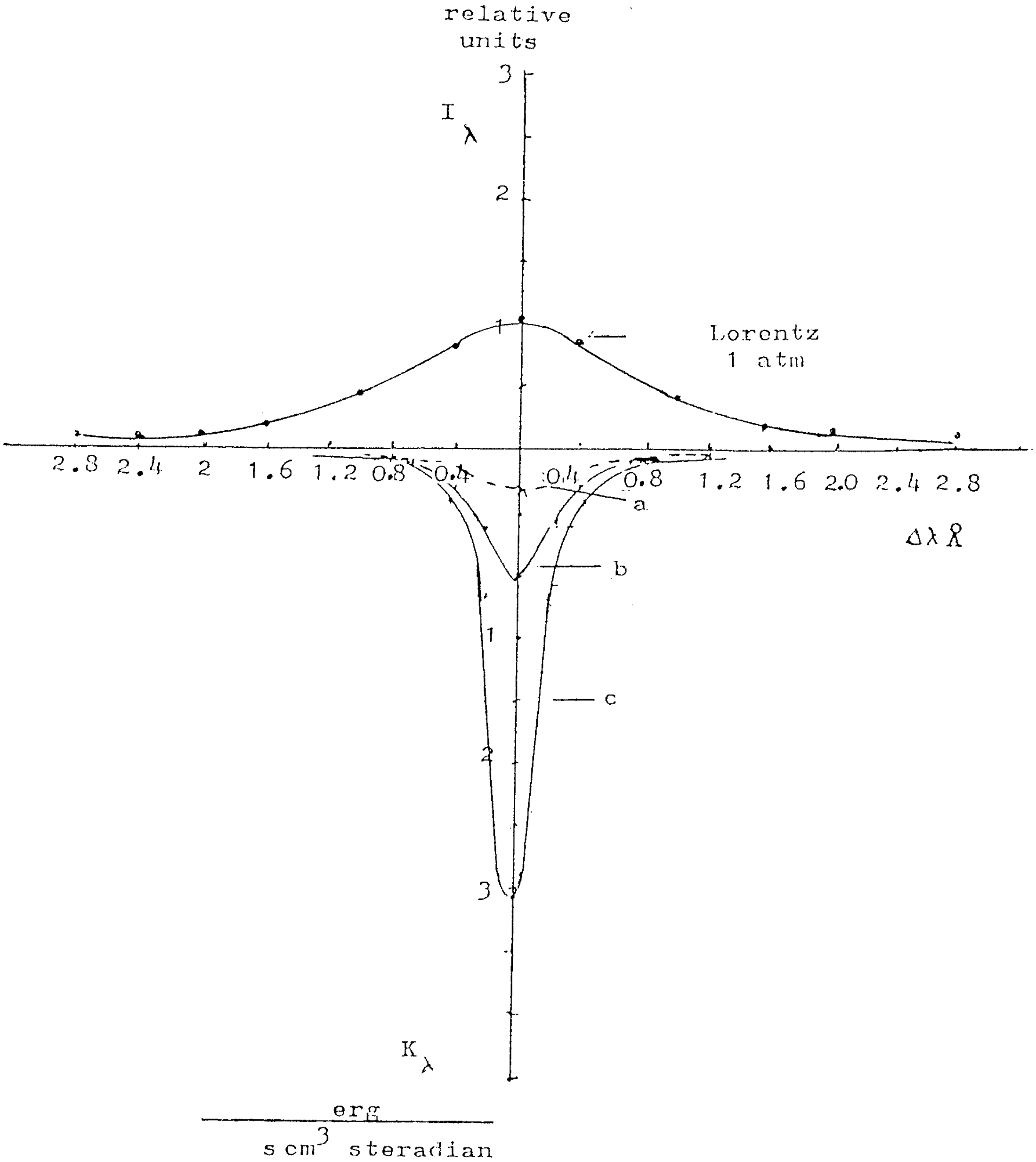

Fig. 2. Line absorption profiles of ArI 4300 Å vs. wavelength $\Delta\lambda$ at 1, 2 and 3 atm (curves a, b and c, respectively) and the Lorentz profile of the emitted line spectrum at 1 atm.

Table 4. Relation between I_λ and $\Delta\lambda$ according to (9).

$\Delta\lambda$, Å	0	0.2	0.4	0.6	0.8	1	1.2	1.4	1.6	2
I_λ	1	0.94	0.8	0.64	0.5	0.39	0.31	0.25	0.2	0.14

The measured profile of the ArI 4300 Å spectral line obtained by the photoelectric method has approximately the same shape as the dispersion profile without shift. Since the line shape is symmetric on both sides of the line intensity λ_o, at $P = 1$ atm with $\Delta\lambda_{1/2} = 1.6$ Å, the dispersion profile equals the Lorentz profile in the emission part. This profile is given by [20]

$$I_\lambda = \frac{I_o}{1 + \left[(\Delta\lambda)/(0.5\Delta\lambda_{1/2})\right]^2}, \tag{8}$$

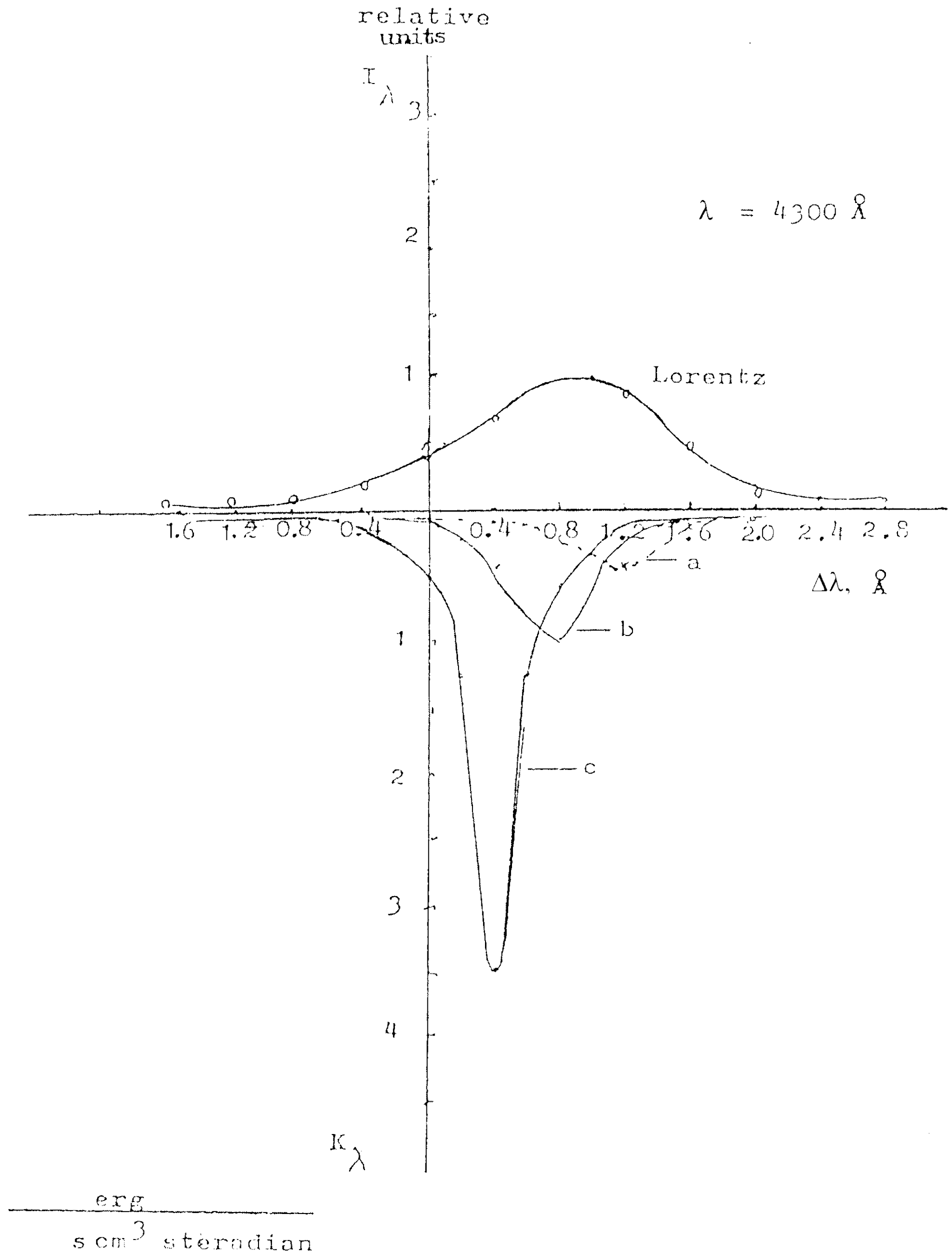

Fig. 3. Line absorption profiles of ArI 4300 Å with shift vs. wavelength $\Delta\lambda$ at 1, 2 and 3 atm (curves a, b and c, respectively) and the Lorentz profile of the emitted line spectrum at 1 atm.

where $\Delta\lambda = (\lambda - \lambda_o - \Delta\lambda_s)$, and the shift $\Delta\lambda_s = 0$. For maximum intensity I_o equals to unity at $\Delta\lambda_{1/2} = 1.6$ Å, and equation (8) takes the form

$$I_\lambda = \frac{I_o}{1 + [(\Delta\lambda)/(0.5 \cdot 1.6)]^2}. \quad (9)$$

Table 4 shows the relation between I_λ (emission) and $\Delta\lambda$ according to (9).

Figure 2 shows the four profiles. The present results show that the experimental shift relative to the half-width $(\Delta\lambda_s/\Delta\lambda_{1/2})$ is 0.74 : 1. Therefore (5), (6), (7) and (9) are rewritten with a shift according to

Hindmarsh [21], where $\Delta\lambda$ is replaced by $(\Delta\lambda - 1.2)$, $(\Delta\lambda - 0.74)$, $(\Delta\lambda - 0.39)$ and $(\Delta\lambda - 1.2)$, respectively. Similarly one can use $\Delta\lambda$ in the relations of K_λ and I_λ.

Figure 3 shows the three profiles with shift under the different pressures plus the Lorentz profile of the emitted line.

4.1. The Quasi-static Approximation

Under 1 atm, the unperturbed spectral line frequency ω_o equals $5 \cdot 10^{10}$ s^{-1}. At 1, 2 and 3 atm, the relative frequency separation $(\Delta\omega_o/\omega_o)$ equals 1, 0.49, 0.2, respectively. The corresponding wavelength separations $\Delta\lambda_o$ are 0.049, 0.024 and 0.0097 Å, respectively, using the relation

$$\Delta\omega_o = \frac{2\pi c}{\lambda^2}\Delta\lambda_o = \frac{1.9 \cdot 10^{19}}{\lambda^2}\Delta\lambda_o.$$

The intensity distribution equation (3) in the three cases becomes

(i) at 1 atm,

$$K_\lambda = 7.6 \cdot 10^{-14} \frac{1}{(\Delta\lambda)^{1.75}} \exp\left[-0.1/(\Delta\lambda)^{0.75}\right], \quad (10)$$

(ii) at 2 atm,

$$K_\lambda = 4.45 \cdot 10^{-14} \frac{1}{(\Delta\lambda)^{1.75}} \exp\left[-0.061/(\Delta\lambda)^{0.75}\right], \quad (11)$$

(iii) at 3 atm,

$$K_\lambda = 2.24 \cdot 10^{-14} \frac{1}{(\Delta\lambda)^{1.75}} \exp\left[-0.031/(\Delta\lambda)^{0.75}\right]. \quad (12)$$

Table 5 and Fig. 4 show the relation between K_λ and $\Delta\lambda$ for the fractional part of (10) – (12).

The measured Stark broadening parameters for ArI 4300 Å agree well with those calculated by Griem [22].

By gas pressure broadening we mean here a collision damping phenomenon, where the motion of the perturbers is treated by a collision mechanism. With the impact approximation, our results show that the group profiles without shifts have a Lorentz shape. This seems to imply that the collisions occur one at a time and are separated by large time intervals. We have attributed the broadening of a line by pressure to the sudden change in phase of the emitted radiation, which is called collision damping. It is assumed that the frequency of the oscillation changes suddenly when the emitting atom is influenced by the colliding atom. After the collision, the original frequency is resumed. The asymmetry and pressure shift are attributed to the modified radiation at the center of the line, as shown in Figure 3. The explanation has been given that at close approach of the rubidium atom the energy levels of the excited Ar atoms are altered due to polarization effects.

Table 5. Relation between K_λ and $\Delta\lambda$ for the fractional part of (10) – (12).

$\Delta\lambda$, Å	0	0.2	0.4	0.6	0.8	1	1.2	1.4	1.6	1.8	2
K_λ	0	12	4.07	2.1	1.3	0.9	0.67	0.51	0.4	0.33	0.28
K_λ	0	13.63	4.4	2.2	1.37	0.94	0.67	0.53	0.42	0.34	0.29
K_λ	0	15	4.67	2.34	1.42	0.97	0.7	0.54	0.43	0.35	0.29

At normal temperature and pressure the collision times are small and the broadening and shift are small too. With increasing pressure the mean collision time increases and the time between successive collisions decreases, with the result that the line is red shifted and broadened asymmetrically. Therefore, the impact approximation is expected to be valid as long as the line widths (and shifts) remain much smaller than the pertuber energies (divided by $h/2\pi$) and the duration of effective collisions is smaller than the times of interest in the Fourier integral describing the line shape [23].

4.2. The Transition between Impact and Statistical Theories

As we pointed out, the basic validity criterion for the impact theory is that the collision time is small compared to the time between impacts. This criterion does not hold in case of sufficiently high particle densities, so that several perturbers are inside the Weisskopf radius. The later naturally dominate the time variation of the perturbing fields, and those of the ion-produced fields can thus not be ignored as long as their time scales are smaller than that caused by the electron impacts. Thus, there are sufficiently large frequency separations $\Delta\omega$ from the line core in the statistical approximation. Radiation at large $\Delta\omega$ can be produced by collisions with small impact parameters ρ_s, during of which the oscillator will radiate at a frequency $\omega = \omega_o + \Delta\omega(\rho_s)$. The intensity of this radiation will be proportional to the statistical frequency of impacts at ρ_s. On the time scale in which the frequency perturbation $\omega_p(t)\left[= \frac{C_n}{r^n}\right]$ and its derivative undergo appreciable relative variations, the right hand side of

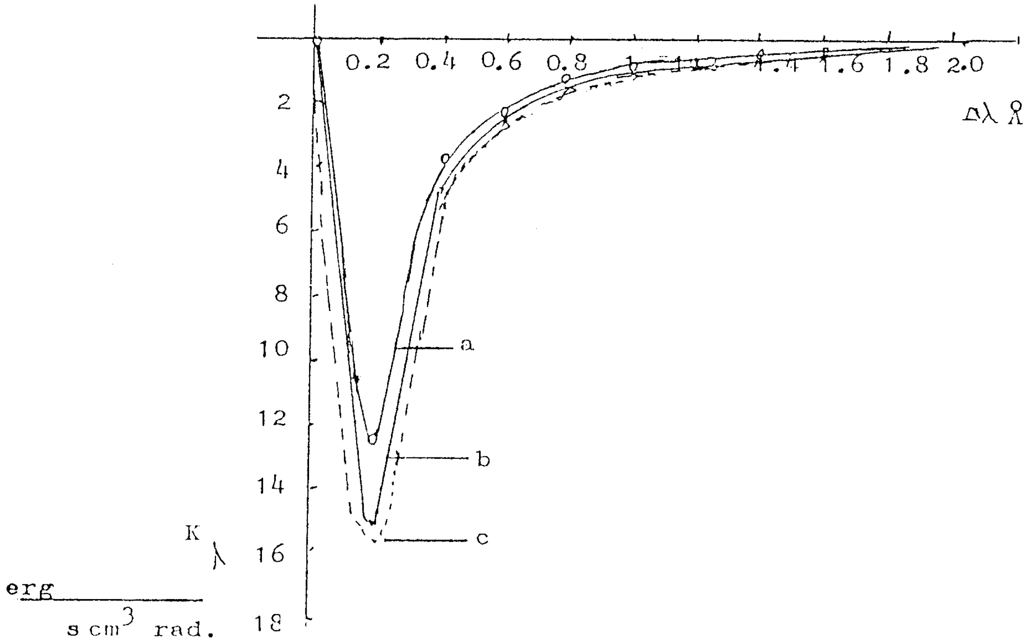

Fig. 4. Fractional drop in the absorption of line ArI 4300 Å vs. wavelength $\Delta\lambda$ at 1, 2 and 3 atm (curves a, b and c, respectively).

(5) drops rapidly to zero except at points, at which $\omega_\mathrm{p}(t) = \omega$, as show the results in Figure 4. Hence, only the neighborhoods of these "coincidence" points contribute significantly to the intensity distribution. So we consider the fractional part of K_λ in Table 5 as equal to the occurrence distribution of $\omega_\mathrm{p}(t)$, i. e. that fraction of the time interval for which $\omega_\mathrm{p}(t)$ is contained in a unit frequency range at ω. The asymptotic behaviour for higher pressures $\Delta\omega_\mathrm{o} \ll \Delta\omega$ is identical, indicating that the strong perturbations are always due to one single Rb perturber atom which is very close to the radiating Ar atoms, as predicted by the proposed assumptions of the statistical treatment equation (3) derived by Unsöld [12].

5. Conclusion

In summary, our detailed discussion of pressure profiles of spectra yields the following general results and conclusions:

• The results of this paper support the assumption that the line width due to collisions varies directly as the pressure.

• The ion densities in electrical discharges and stars are often determined by observing the widths of spectral lines emitted or absorbed. Pressure profiles are usually employed in the interpretation of the data.

• The Lorentzian profile is very useful for the interpretation of electronic line shapes in pressure profile formations.

• This study is important for the spectral analysis of alkali metals which are evaporated in an arc.

Acknowledgements

The experimental facilities provided by Prof. J. Richter, Kiel University, Germany are highly appreciated. We are grateful to Prof. A. A. El-Attar, Physics Department, Assiut University, Egypt for reading the manuscript.

[1] W. Watson and H. Margenau, Phys. Rev. **44**, 748 (1933).
[2] T. Z. Ny and S. Y. Ch'en, Phys. Rev. **52**, 1158 (1937).
[3] J. Robin and S. Robin, Compt. Rend. **233**, 1019 (1951).
[4] C. Gregory, Phys. Rev. **61**, 465 (1942).
[5] J. Tomiser, Acta Phys. Austria **8**, 328 (1954).
[6] H. Kusch and W. Schreiber, Z. Physik **255**, 257 (1972).
[7] N. Nessib, Z. B. Lakhdar, and S. Sahal-Brechot, Phys. Scr. **54**, 608 (1996).
[8] S. H. Zaidi, Z. Tang, and R. B. Miles, 28th IEEE Intern.

Conf. on Plasma Science and 13th IEEE Intern. Pulsed Conf., Las Vegas, NV, USA, 246 (2001).

[9] S. T. Cundiff and J. M. Shacklette, 12th Intern. Conf. on Ultrafast Phenomena, Technical Digest, Postconference Edition, Carleston, SC, USA, **43**, 262 (9 – 13 July 2000).

[10] S. Dijurovic, D. Nikolic, Z. Mijatovic, R. Kobilarov, and N. Konjevic, 25th ICPIG (Intern. Conf. on Phenomena in Ionized Gases), Nagoya, Japan, **4**, 9 (17 – 22 July, 2001).

[11] V. Helbig and H. Kusch, Astro. Phys. **120**, 299 (1972).

[12] A. Unsöld, Physik der Sternatmosphären, Springer-Verlag, Berlin 1968.

[13] H. R. Griem, M. Baranger, A. C. Kolb, and G. Oretel, Phys. Rev. **125**, 177 (1961).

[14] E. D. Clayton and S. Y. Ch'en, Phys. Rev. **85**, 68 (1952).

[15] D. Mihalas, Stellar Atomspheres, Burbidge 1970.

[16] P. W. Anderson, Phys. Rev. **76**, 647 (1949).

[17] W. L. Wiese, D. E. Kelleher, and V. Helbig, Phys. Rev. **11A**, 1854 (1975) (cf. Fig. 1).

[18] T. L. Pittman and C. Fleurier, in: Spectral Line Shapes, Vol. **2** (Ed. K. Burnett), de Gruyter, New York 1983.

[19] J. Shumaker, J. Res. A. Phys. & Chem. **76A**, 72 (1971).

[20] Z. A. All, Ph. D. Thesis, Assiut University, Assiut, Egypt 1987.

[21] W. Hindmarsh, Collision Broadening of Spectral Lines by Neutral Atoms, Pergamon Press, Elmsford, New York 1972.

[22] H. R. Griem, Phys. Rev. **128**, 515 (1962).

[23] H. R. Griem, Spectral Line Broadening by Plasmas, Academic Press, New York 1974.